


# Water and oil signal assignment in low-moisture mozzarella as determined by time-domain NMR $T_2$ relaxometry

Lien Vermeir<sup>1</sup>  | Arnout Declerck<sup>1</sup> | Chak Ming To<sup>2</sup> | Barbara Kerkaert<sup>2</sup> | Paul Van der Meeren<sup>1</sup>

<sup>1</sup>Particle and Interfacial Technology Group, Department of Green Chemistry and Technology, Faculty of Bioscience Engineering, Ghent University, Ghent, Belgium

<sup>2</sup>Milcobel cbva, Industrial Products Division, Kallo, Belgium

## Correspondence

Lien Vermeir, Particle and Interfacial Technology Group, Faculty of Bioscience Engineering, Ghent University, Coupure Links 653, Ghent B-9000, Belgium.  
Email: [lien.vermeir@ugent.be](mailto:lien.vermeir@ugent.be)

## Funding information

Flanders Innovation & Entrepreneurship (VLAIO), Grant/Award Number: HBC.2017.0297

## Abstract

A time-domain  $^1\text{H}$  nuclear magnetic resonance relaxometry method was elaborated for the rapid microstructural characterization of mozzarella cheese. For this purpose, there is a strong need to know how the experimentally determined  $T_2$  relaxation time distribution can be related to specific constituents in mozzarella. In this study, a detailed investigation is offered for fresh and aged low-moisture mozzarella cheese, often applied as a pizza cheese, by application of both a conventional Carr–Purcell–Meiboom–Gill (CPMG) sequence and a free-induction decay CPMG (FID-CPMG) sequence. The relaxation behavior was further elucidated by addition of deuterium oxide and by mild heat treatment of samples. The relaxation times of water protons in mozzarella were found to range from a few microseconds to some tens of milliseconds (in aged mozzarella) or to about hundred milliseconds (in fresh mozzarella). The upper limit of the  $T_2$  distribution can even be extended to the seconds range upon releasing water protons from the mozzarella matrix using a mild heat treatment or upon addition of deuterated water. Both stimuli also provided evidence for the absorption of water into the cheese matrix. The potential release and uptake of water demonstrated that mozzarella acts as a very dynamic system during production and storage. The detected differences in the behavior of the water fraction between fresh and aged low-moisture mozzarella might be utilized to study the influence of either production and/or storage conditions on the cheese ripening process.

## KEYWORDS

CPMG, FID-CPMG,  $^1\text{H}$ , low-field NMR, mozzarella, NMR,  $T_2$  relaxation, time-domain NMR

## 1 | INTRODUCTION

Pasta filata mozzarella cheese is obtained as a result of a complex process that incorporates a number of steps, including renneting, stretching, and salting. During the former step, rennet is added to the milk, whereby the proteolytic enzymes of the rennet transform the milk into curds and whey. Subsequently, the curds are diced,

cooked, and stretched. The stretching process results in orientation of the protein fibers between which water and fat reside.<sup>[1]</sup> Salting of mozzarella improves the microbiological stability, flavor, and texture.

Different techniques have been described for studying the microstructure of mozzarella. Microscopic techniques, such as confocal laser scanning microscopy and cryo-scanning electron microscopy, have been applied to

monitor the effect of aging<sup>[2–4]</sup> or different process and recipe conditions on the microstructure.<sup>[5–8]</sup> Prior to imaging, dyes are required to visualize the fat and protein matrix using confocal laser scanning microscopy and cryofixation is needed for cryo-scanning electron microscopy, which might create artefacts.<sup>[9]</sup> Less sample preparation is needed to explore various states of water using differential scanning calorimetry (e.g., for determination of the freezable water) or a centrifugation method. Water in freshly produced mozzarella is freely available in the fat-serum channels interspersed throughout the protein matrix and may be expressed by centrifugation (i.e., the so-called expressible water).<sup>[10]</sup> Upon aging of mozzarella, the water-binding capacity increases, by which the fraction of expressible water decreases.<sup>[10–12]</sup>

In the last decades, time-domain <sup>1</sup>H nuclear magnetic resonance (NMR) has been suggested as a complimentary technique, with the main advantages that it is a fast method and it does not require any sample pretreatment. Two main NMR techniques have been described to collect information on the most abundant constituents in mozzarella (e.g., water and lipids), that is, diffusometry and relaxometry.

Time-domain NMR water diffusometry is concerned with the quantitative determination of the water self-diffusion coefficient in a sample by evaluating the self-diffusion decay rate. The self-diffusion of water molecules is impeded by macromolecules due to both the required diversion to diffuse around the macromolecule and the momentary inhibition caused by interaction with the macromolecule. This method has been applied for comparison of unfrozen mozzarella and thawed samples after freezing.<sup>[13]</sup>

Time-domain NMR T<sub>2</sub> relaxometry is concerned with the quantitative determination of the relaxation components of a sample by evaluating the magnetization decay rates and amplitudes of the NMR signal. The T<sub>2</sub> relaxation time of water and lipids, a measure for the decay rate, depends on the structural environment (e.g., in a pore or within fat globules) and the physical state (liquid or solid). Furthermore, water relaxation is affected by exchange between water protons and exchangeable protons on small solutes or macromolecules (which usually have a shorter relaxation time). Consequently, the relaxation curves for cheese usually show a multiexponential behavior. Hereby, the relaxation time of water in cheese is usually shorter as compared with the corresponding relaxation time in bulk water. For this reason, this technique has been applied to study the water distribution in food<sup>[14–16]</sup> and to monitor water loss during brining of cheese.<sup>[17]</sup>

The objective of this study was to aid the interpretation of the T<sub>2</sub> relaxation time distribution of fresh and aged

mozzarella as obtained by applying a Carr–Purcell–Meiboom–Gill (CPMG)<sup>[14,18–21]</sup> and free-induction decay CPMG NMR (FID-CPMG NMR) sequence.<sup>[21]</sup> Furthermore, addition of D<sub>2</sub>O and a mild heat treatment were applied to further elucidate the relaxation behavior.

## 2 | EXPERIMENTAL

### 2.1 | Materials

Commercial blocks (about 28 × 10 × 8 cm) of 2.5-kg low-moisture mozzarella were manufactured by Milcobel (Langemark, Belgium), which consisted of 47% water, 22.6% fat, 25% protein, 1.5% salt, and 4% other compounds. Hence, the fat in dry matter content was about 43%. The vacuum-packed blocks were stored for less than 1 day (fresh) or for 1 month (aged) at 4°C.

Deuterated water (with a purity of 99.8% atom %D) was purchased from Armar Chemicals (Switzerland). Diethyl ether, sodium chloride, and anhydrous sodium sulfate were obtained from VWR Chemicals (Leuven, Belgium). The 0.1-M phosphate buffer (pH 7) contained KH<sub>2</sub>PO<sub>4</sub> (Merck KGaA, Darmstadt, Germany) and K<sub>2</sub>HPO<sub>4</sub> (Alfa Aesar, Karlsruhe, Germany). All above-mentioned chemicals were reagent grade and used without further purification.

### 2.2 | Extraction procedures

Bulk mozzarella serum was obtained upon mildly heating fresh mozzarella for 1 hr at 30°C.

The extracted fat phase (EFP) of mozzarella was obtained upon mixing the mozzarella with diethyl ether and filtering over anhydrous sodium sulfate. The ether was then removed using a rotary evaporator (Heidolph, Germany) at 55°C.

### 2.3 | NMR sample preparation

For most experiments, fluorinated ethylene propylene NMR open tubes (180 mm length, 16 mm inner diameter, 1 mm wall thickness) were pushed into the central part of an aged block with about 6 cm intertube spacing, resulting in cylindrical mozzarella samples of about 80 mm height and about 16 mm diameter. The fluorinated ethylene propylene tubes were closed at both sides using Teflon plugs; the bottom plug contained an air channel, which was sealed with Vaseline against dehydration of the sample.

For experiments on the EFP, cylindrical samples were obtained using a cheese trier and transferred into a glass

NMR tube (18 mm O.D., 15.2 mm I.D., Oxford Instruments, UK). This sampling procedure was also used for mozzarella samples to be subjected to a mild heat treatment or to mozzarella samples submerged in (normal or heavy) water. In the latter case, the aged mozzarella cylinders (14 mm diameter and about 80 mm height) were placed in a glass NMR tube (18 mm O.D., 15.2 mm I.D., Oxford Instruments, UK) and completely submerged in a H<sub>2</sub>O or D<sub>2</sub>O phase, which consisted of 1.5% (w/v) NaCl in a 0.1-M phosphate buffer (pH 7).

## 2.4 | Time-domain NMR measurements

Low-field NMR measurements were performed on a benchtop Maran Ultra spectrometer (Oxford Instruments, Abingdon, UK) operating at 0.55T (23.4 MHz for <sup>1</sup>H). Two NMR sequences were employed: the CPMG<sup>[22]</sup> and the FID-CPMG sequence. Short time scales of the relaxation decay (<50 μs) are only accessible using an FID sequence, which results in a T<sub>2</sub>\* relaxation time distribution due to solid phase protons (e.g., protons of the solid fraction of the fat phase in cheese).<sup>[23]</sup> The CPMG sequence provides details about the T<sub>2</sub> relaxation time of protons from the liquid phase (i.e., T<sub>2</sub> > 100 μs). Combining both sequences into one (FID-CPMG) sequence may yield the relaxation time distribution of solid phase and liquid phase protons. Hereby, T<sub>2</sub>\* is mostly shorter than T<sub>2</sub> due to effects of magnetic field inhomogeneity and can be considered as an apparent T<sub>2</sub>.<sup>[24]</sup>

Regarding the CPMG and FID-CPMG sequence, each measurement was acquired using a 90° pulse (7.3 ms) and 180° pulse (14.6 ms), whereas a 2τ interpulse spacing of 0.18 and 0.30 ms was applied for the CPMG and FID-CPMG sequence, respectively. The latter value was the lowest possible setting using the FID-CPMG sequence on the available NMR spectrometer. For measurement of the aged mozzarella and the EFP at 5°C, the recycle delay (RD), the number of scans, and the number of echoes were set at 2 s, 16, and 4,096, respectively. As there is a direct relationship between sample temperature and T<sub>1</sub> relaxation time, the RD (with RD = 5·T<sub>1</sub> as a rule of thumb) was set slightly higher (4 s) for measurement of the EFP at 15°C. The number of echoes and the RD were increased to 8,192 and 10 s, respectively, for analysis of fresh mozzarella, bulk mozzarella serum, and tubes containing D<sub>2</sub>O or H<sub>2</sub>O phase (at 5°C). The larger settings were needed because of the presence of water, which has a longer T<sub>1</sub> relaxation time.

For each condition, NMR measurements were made in triplicate and results are expressed as a mean value with its standard deviation.

## 2.5 | CPMG and FID-CPMG fitting procedure

Upon performing an FID-CPMG or CPMG experiment, an exponentially decaying curve is obtained. A fitting procedure is applied to obtain the T<sub>2</sub> relaxation time for each relaxation component from the FID-part and CPMG-part of the relaxation curve.

Taking into account that water and oil molecules in heterogeneous food systems may be characterized by several relaxation times, a full assessment of water and oil properties is only possible using a technique that can fit the data into a continuous spectrum of relaxation times.<sup>[25]</sup>

Using the WinDXP software (version 1.8.1.0, Oxford Instruments, UK), CONTIN analysis was applied to the CPMG data,<sup>[26,27]</sup> which determines the number of proton pools (*H*) and their corresponding intercepts (*I*) for a distribution of relaxation times (T<sub>2</sub>). To speed up the fitting procedure, the large data set of echo points was pruned to 256 prune points set on a logarithmic basis.

Regarding the FID-CPMG data, a simplified version of CONTIN in MATLAB (version 9.3.0.713579, R2017b, The MathWorks) was applied. Using the rilt.m-file (regularized inverse Laplace transform), the number of proton pools (*H*) and their corresponding intercepts (*I*) for a distribution of relaxation times (T<sub>2</sub>\* and T<sub>2</sub>) are determined. Hereby, the CPMG-part (which starts at 304 μs) of the FID-CPMG signal was described by a set of 50 exponential functions, whereas the FID-part (which ends at 118 μs) was described by a set of 50 Gaussian functions (Equation 1).

$$\text{Relaxation magnitude}_{\text{FIDCPMG}}(t) = \sum_{i=1}^{50} I_i \cdot e^{-0.5 \left( \frac{t}{T_{2,i}} \right)^2} + \sum_{j=1}^{50} I_j \cdot e^{-\frac{t}{T_{2,j}}} \quad (1)$$

In case the T<sub>2</sub>(\*) relaxation time distribution, represented by *I* (T<sub>2</sub>(\*)), is characterized by multiple peaks, each relaxation component or peak was characterized by the T<sub>2</sub>(\*) value at maximum signal amplitude, as well as by the integrated signal amplitude *A* (or peak area). Hereby, *A* quantifies the fraction of protons with T<sub>2</sub>(\*) values that are covered by a specific relaxation peak. Dividing the *A* value by the sample mass, the mass-normalized peak area (*A<sub>m</sub>*) is obtained. As an example, the mass-normalized peak area of the weakly interacting water in fresh mozzarella corresponds to

$$A_{m, \text{ water in fresh mozz}} = \sum_{T_{2,k}=60}^{2 \text{ s}} \frac{1}{m_{\text{sample}}} I_k(T_{2,k})$$

The FID-CPMG experiment can be applied to determine the solid fat content using Equation (2). Liquid oil protons usually contribute to the CPMG-part of the T<sub>2</sub>

signal at  $T_2 > 100 \mu\text{s}$ , whereas solid fat protons can be measured at the FID-part at a  $T_2^* < 26 \mu\text{s}$ . A  $T_2^*$  between 50 and  $250 \mu\text{s}$  has been assigned to an intermediate phase between the liquid and the solid phases.<sup>[21,24]</sup>

$$\text{SFC (\%)} = \frac{A_{\text{FID, solid fat}}}{A_{\text{FID, solid fat}} + A_{\text{CPMG, liquidoil}}} \times 100\%. \quad (2)$$

### 3 | RESULTS AND DISCUSSION

#### 3.1 | Discrete and multiexponential fitting of CPMG data

Many applications of the CPMG sequence for analysis of cheese have been described.<sup>[18,20,28–34]</sup> Some NMR relaxometry studies focused on mozzarella.<sup>[4,11,14,19,35–37]</sup> Mozzarella with a high fat in dry matter content (FDM of about 50%) was investigated by Gianferri et al.,<sup>[14]</sup> Baranowska et al.,<sup>[36]</sup> Cais-Sokolinska et al.,<sup>[19]</sup> and Smith

et al.,<sup>[4]</sup> and these studies applied a low-field NMR spectrometer and a continuous multiexponential model fitting, whereas the latter study used a high-field NMR device. Hereby, the obtained relaxation components were attributed to specific proton pools but clearly depended on the applied cheese formulation and the experimental setup. Mostly, at least two water relaxation components were found,<sup>[19,36]</sup> whereas Gianferri et al.<sup>[14]</sup> reported on three water relaxation (at 7, 16 and 488 ms) and one fat relaxation component (at 69 ms). In some studies, chemical shift-resolved water signals were obtained for mozzarella with a FDM of about 40%.<sup>[11,35,37]</sup> Hereby, a discrete biexponential fitting to the water signal was applied, resulting in a fast water component at 7.5 ms and a slower water component at 20 ms at 5°C.<sup>[11]</sup>

Regarding our CPMG data of mozzarella with an FDM of 43%, a poor fitting of the discrete biexponential model was obtained for data below 1 ms, whereas a continuous multiexponential fitting (second term of Equation 1) resulted in better results (Figure 1b).

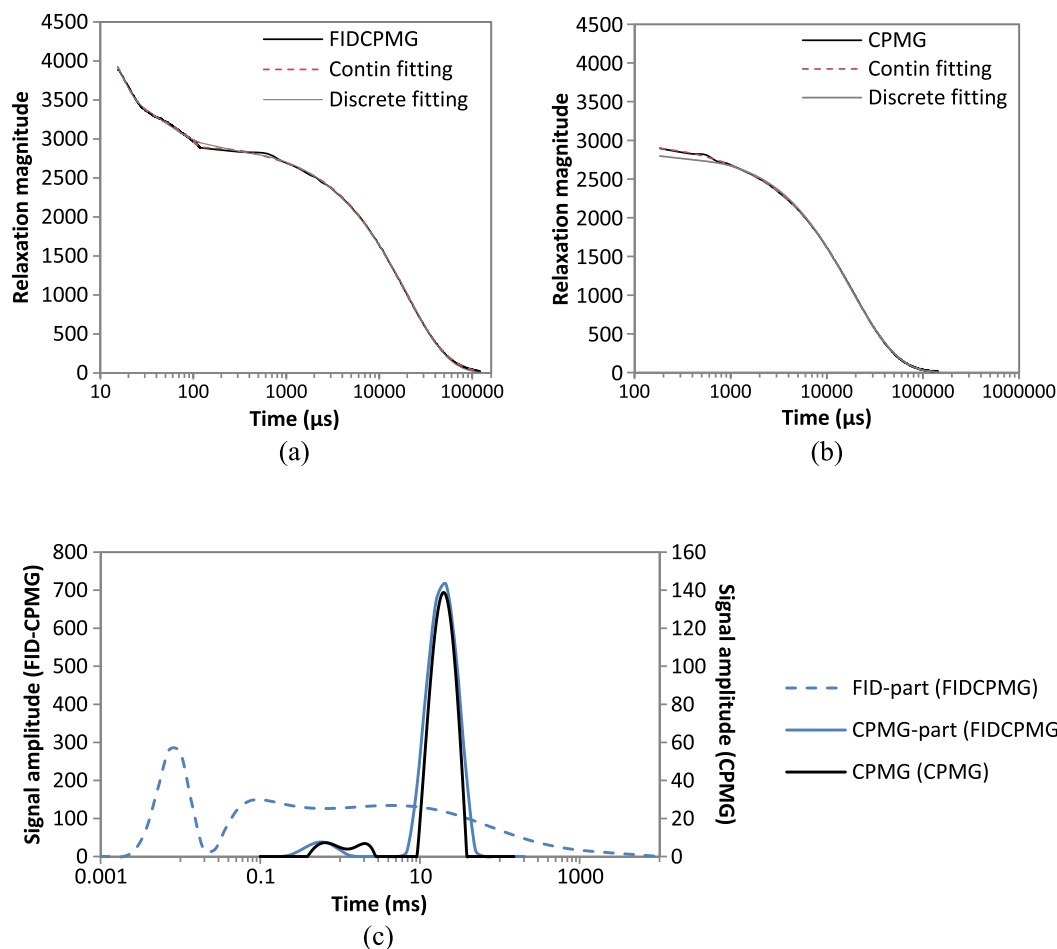


**FIGURE 1** Fitting of the (a) free-induction decay Carr–Purcell–Meiboom–Gill (FID-CPMG) and (b) CPMG relaxation magnitude of aged mozzarella (black line) using discrete (grey line) and nondiscrete (CONTIN, dashed red line) fitting procedure. (c) The resulting best fitted FID-based  $T_2^*$  (dashed line) and CPMG-based  $T_2$  (full lines) relaxation time distribution using CONTIN analysis. The blue lines and black line refer to two distributions as obtained from the FID-CPMG sequence and to the results from the CPMG sequence, respectively



### 3.2 | Discrete and multiexponential fitting of FID-CPMG data

The FID-CPMG sequence was applied to gather information at a shorter time scale, which might aid to interpret the CPMG-based relaxation time distribution and, hence, to assign different relaxation components to particular proton pools. To our knowledge, only Chaland et al.<sup>[21]</sup> have applied both the FID and the CPMG sequence for analysis of soft and hard cheeses, after which the signals were fused and fitted using a discrete least-squares (Marquardt) fitting procedure whereby the solid part was described by a Gaussian (at 14.5  $\mu$ s) and an exponential component (at 90  $\mu$ s) and the liquid part by a biexponential function (at 7 and 43 ms). The application of this model to our FID-CPMG data generated a poor fitting at the FID-CPMG junction and at the CPMG-signal tail (Figure 1a), whereas CONTIN analysis resulted in a better model fitting.

The resulting  $T_2^*$  and  $T_2$  relaxation time distributions for the studied mozzarella at 5°C are shown in Figure 1c. Using the FID data (dashed line in Figure 1c), a peak at about 8  $\mu$ s was found, as well as a broad peak covering a range of  $T_2^*$  times much longer than 118  $\mu$ s. Whereas the former is due to solid-like protons of the fat, the latter is due to liquid-like protons (from liquid oil and water). As compared with the CPMG data (full lines in Figure 1c), the broad peak is expected to yield less reliable information about protons from the liquid phase, because the FID data were acquired only up to 118  $\mu$ s. Hence, this second peak in the FID-based  $T_2^*$ -distribution will not be discussed in great detail.

Two (a minor and a major) peaks at about 1 and 20 ms were obtained from the CPMG-part of the FID-CPMG sequence, which corresponded to the relaxation components obtained from the CPMG experiment only. The major peak is in agreement with the dominant component at 16 ms for freshly prepared mozzarella di Bufala Campana at 8°C (FDM of about 50%),<sup>[14]</sup> but in contrast with the dominant component at 7.5 ms (and a minor component at 20 ms) for freshly prepared mozzarella at 5°C (FDM of about 40%).<sup>[11]</sup> The disagreement might be explained by the difference in cheese recipe, as well as by the shorter relaxation decay employed in the latter study.<sup>[11]</sup>

### 3.3 | Assignment of relaxation components to particular proton pools in mozzarella

In order to assign relaxation peaks to the main mobile cheese constituents (i.e., water and the liquid fraction of

the fat phase), four approaches are presented. First, the chemical composition of mozzarella was used to elucidate the relaxation behavior, whereby it was assumed that each peak in the relaxation distribution may be linked to an individual cheese constituent. Second, the relaxation profile of mozzarella and of the EFP was compared to provide insight into the contribution of oil protons to the cheese relaxation profile, supposing that the fat phase in bulk and within cheese behaves similarly. Furthermore, the measurement of the EFP at two sample temperatures enables evaluating changes in the relaxation time distribution following a transition from solid fat to liquid oil. Third, the contribution of water protons to the mozzarella relaxation profile was evaluated upon comparison of fresh mozzarella before and after application of a mild heat treatment for 1 hr at 30°C. Hereby, some serum is released from the heated mozzarella. As water protons in the released serum experience much less interactions with the cheese matrix, a new peak (with a longer relaxation time) is expected to appear. Simultaneously, the original water populations are expected to decrease. Exchange between different water populations might also be brought about upon addition of deuterated water to aged mozzarella. These different approaches are discussed into more detail in the following subsections.

### 3.4 | The chemical composition of mozzarella

Gianferri et al.<sup>[14]</sup> applied the CPMG sequence and assigned the four relaxation components in mozzarella to three types of water protons and fat protons. The latter was assigned on the basis of the composition of mozzarella cheese with 54–60% water and 20–25% lipids. Whereas the relaxation time of solid fat protons is too short to be measured by a CPMG sequence,<sup>[23]</sup> the protons of water and of the liquid fraction of the fat phase are supposed to be sufficiently mobile to contribute to the CPMG relaxation signal. At 5°C, a milk fat phase consists of only about 40% liquid oil protons.<sup>[38]</sup> Hence, the contribution of the lipid phase can only represent about 15% of the CPMG signal, whereas a contribution of 27% (to a single component) was reported.<sup>[14]</sup> Furthermore, the hypothesis that each component in the relaxation profile might be linked to an individual cheese constituent might not be valid when, for example, oil protons—with a broad oil relaxation time distribution—contribute to the water proton populations.<sup>[21,30]</sup> In addition, protein protons might also contribute to the CPMG profile, although precise analysis and identification of a specific relaxation time was not possible using a low-field NMR spectrometer.<sup>[21]</sup>

### 3.5 | EFP of mozzarella

The contribution of oil protons to the cheese relaxation profile has been investigated by comparison of profiles of cheeses with different fat content,<sup>[18–21]</sup> fat-free cheese,<sup>[28]</sup> or bulk fat at the same sample temperature.<sup>[21,28]</sup> As water does not interact with the lipid component, a decrease or increase in fat content is not expected to affect the relaxation time distribution of the water protons.<sup>[14]</sup>

In this study, the  $T_2$  relaxation time profiles of the EFP and aged mozzarella were compared (Figure 2a,b and Table 1). A difference in spatial distribution of the fat phase (i.e., distributed as fat channels in aged cheese<sup>[4]</sup> vs. bulk fat phase) might affect the solid fat content and the relaxation time of the fat phase. Nevertheless, this experiment provides information about the relevance of the fat phase proton population and its approximate relaxation time in mozzarella.

As similar CPMG-results on EFP were obtained using the FID-CPMG and CPMG sequence, and additional relaxation information at a shorter time scale was required, mainly the former sequence was applied hereafter.

Using the results from the FID-CPMG experiment (Table 1) and using Equation (2), the solid fat content of the bulk EFP at 5°C amounted to 69%. Assuming a similar solid fat content (SFC), the mass-normalized contribution of solid fat is expected to be 198 g<sup>-1</sup> mozzarella. However, the experimentally determined value ( $A_m = 129$  g<sup>-1</sup>) corresponds with a SFC of 45% in mozzarella. It is known that the SFC of bulk fat might differ from that of emulsified fat.<sup>[39]</sup> Based on 22.6% fat in mozzarella, 12.6% of liquid oil (and 10% of solid fat) is expected in the analyzed sample.

The smaller FID-relaxation peak of mozzarella and EFP at a  $T_2^*$  between 26 and 150  $\mu$ s is in agreement with an amorphous fraction of the fat phase.<sup>[21]</sup> This proton pool is hereafter referred to as  $H_{\text{amorphous fat}}$ .

Regarding the results from the CPMG-part of the FID-CPMG experiment in Figure 2b, it is assumed that water (47% in mozzarella) and liquid oil (about 13% in mozzarella) are CPMG-detectable, so that the signal for mozzarella should be built up of protons coming from 78% water and 22% oil. Hereby, the EFP-oil seems to contribute to the complete relaxation time range of mozzarella. This is in agreement with a broad distribution,<sup>[21,30]</sup> which follows from the heterogeneous milk fat phase composition; the relaxation times depend on the length of the carbon chain and the number of chain unsaturations in the fat phase. Hereby, mozzarella and EFP seem to have a similar dominant peak at about 20 ms. Hence, the latter relaxation component for mozzarella is clearly associated with oil protons, as well as with a (much) larger fraction of non-oil protons.

As compared with the total integrated CPMG-signal amplitude of mozzarella ( $A_m = 348$  g<sup>-1</sup> in Table 1), the total signal of 22.6% EFP ( $A_m = 89$  g<sup>-1</sup>) contributes for about 26%, which is slightly higher than the expected 22% oil contribution. The  $A_m$  value for bulk serum amounted to  $568 \pm 3$  g<sup>-1</sup> (CPMG data not shown). The studied mozzarella consisted of about 47% of water (or  $A_m = 267$  g<sup>-1</sup>), which corresponds to a water contribution of about 77% to the experimentally determined value for mozzarella. The latter value is close to the expected 78% water contribution.

Increasing the temperature of bulk fat provides additional information about the contribution of (oil) protons to the cheese relaxation profile. A decrease in solid fat content is expected (and hence, a decrease in the area of

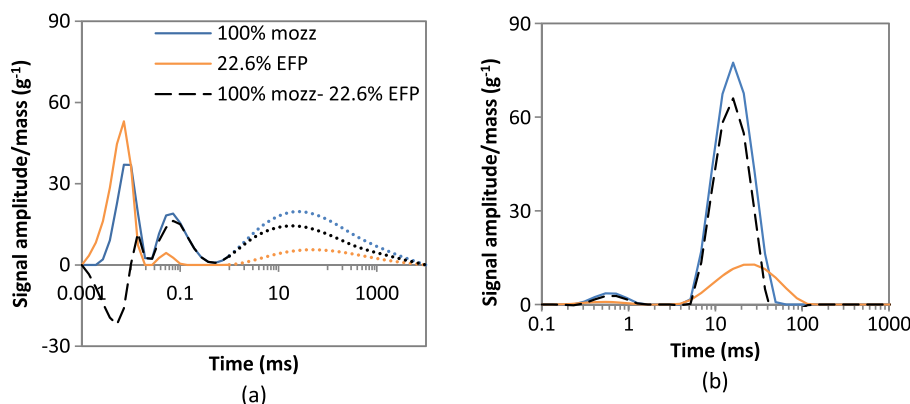


**FIGURE 2** (a) Mass normalized free-induction decay (FID)-based  $T_2^*$  and (b) Carr–Purcell–Meiboom–Gill (CPMG)-based  $T_2$  relaxation time distribution characteristics of aged mozzarella (blue line) and 22.6% of extracted fat phase (EFP; orange line), as well as their subtracted distribution (dashed line), as obtained using the FID-CPMG sequence at 5°C and using CONTIN fitting. FID-dotted lines are less reliable because the time window was limited to 118  $\mu$ s during FID data acquisition

**TABLE 1** Mass normalized integrated signal amplitude ( $A_m$ ) as obtained from the FID and CPMG-part of the FID-CPMG experiment upon CONTIN analysis

Sample	$A_m$ (a.u.)				
	Based on the FID-part		Based on the CPMG-part		
	$T_2^* < 26 \mu\text{s}$	$26 \mu\text{s} < T_2^* < 150 \mu\text{s}$	$T_2 < 3 \text{ ms}$	$T_2 > 3 \text{ ms}$	Total
Mozzarella (5°C)	$129 \pm 7$	$87 \pm 8$	$13 \pm 5$	$335 \pm 54$	$348 \pm 59$
EFP (5°C)	$876 \pm 14$	$45 \pm 3$	$17 \pm 10$	$378 \pm 2$	$395 \pm 12$
EFP (15°C)	$685 \pm 14$	$42 \pm 13$	$23 \pm 9$	$549 \pm 2$	$572 \pm 8$

Note. FID: free-induction decay; CPMG: Carr–Purcell–Meiboom–Gill; EFP: extracted fat phase.

the FID-peak related to the solid fraction of the fat phase), which should result in the detection of more liquid oil protons (and hence, an increase of the associated area of the CPMG-peak).

The EFP sample was heated from 5°C to 15°C (Figure 3 and Table 1). Using the FID-CPMG sequence and Equation (2), the solid fat content of the EFP at 15°C amounted to 54%, which is in the range of SFC reported for milk fat.<sup>[38]</sup> The area of the FID-peak at  $T_2^* < 26 \mu\text{s}$  decreased from 5°C to 15°C (Figure 3a), whereas the peak area at  $T_2^* > 700 \mu\text{s}$  increased with increasing temperature. The latter increase in signal was similar to the increase in total CPMG signal. Hence, evidence is provided that solid fat protons contributed to the relaxation peak at  $T_2^* < 26 \mu\text{s}$  (“ $H_{\text{solid fat}}$ ”) and liquid oil protons must contribute to a broad relaxation time range of the CPMG-signal (“ $H_{\text{liquid oil}}$ ”). The  $A_m$  value of  $H_{\text{amorphous fat}}$  did not change.

In general, heating of a sample results in an increase of its relaxation time(s) through an increase in the rotational mobility of protons. From 5°C to 15°C, the relaxation time of the dominant FID-peak  $H_{\text{solid fat}}$  (Figure 3a) increased from  $6.0 \pm 0.2$  to  $7.0 \pm 0.2 \mu\text{s}$ ; the relaxation

time of the dominant CPMG-peak at  $T_2 > 3 \text{ ms}$  (Figure 3b) increased (albeit not significantly) from  $28 \pm 35$  to  $58 \pm 168 \text{ ms}$ .

### 3.6 | Mild heat treatment of mozzarella

Heating of mozzarella induces multiple changes, which complicates the interpretation of the relaxation time profiles of mozzarella as recorded at different temperatures.

First, an increase in  $T_2$  relaxation time of all proton groups is expected upon increase of temperature, which is mostly explained by the inverse proportionality between the absolute temperature and the correlation time  $\tau_c$ , the time required for the molecule to rotate by approximately one radian. A linear relationship exists between  $\tau_c$  and the  $T_2$  relaxation time.<sup>[40]</sup> Second, in the absence of phase transitions over the considered temperature range (e.g., for water protons), a decrease in signal amplitude is expected due to the inherent decreasing effect of increasing temperature on the NMR signal.<sup>[41]</sup> In the presence of a phase transition (e.g., for solid fat protons), an additional decrease of the signal amplitude

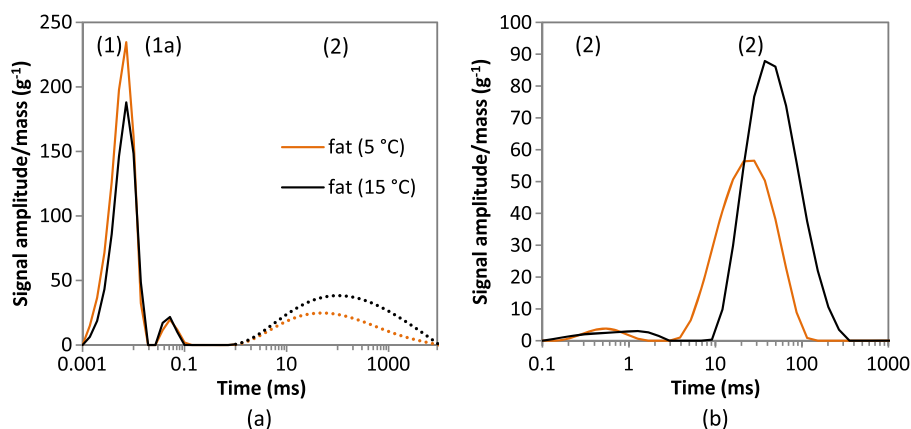


**FIGURE 3** (a) Mass normalized free-induction decay (FID)-based  $T_2^*$  and (b) Carr–Purcell–Meiboom–Gill (CPMG)-based  $T_2$  relaxation time distribution characteristics of extracted fat phase at 5°C (orange line) and at 15°C (black line) as obtained using the FID-CPMG sequence and fitting using CONTIN analysis. FID-dotted lines are less reliable because the time window was limited to  $118 \mu\text{s}$ . 1 =  $H_{\text{solid fat}}$ ; 1a =  $H_{\text{amorphous fat}}$ ; 2 =  $H_{\text{liquid oil}}$

associated with solid fat protons is expected. Third, mild heating of freshly produced mozzarella yields some release of free water. The latter originates from the strengthening of hydrophobic interactions within the protein matrix, which causes the casein matrix to contract and to force some of the water out of the matrix.<sup>[35,37]</sup> However, the interpretation is drastically facilitated when the relaxation signals of fresh mozzarella are recorded at the same temperature (5°C), before and after mild heating for 1 hr at 30°C. The only change that should then be considered is the release of serum. A new peak related to the protons of the released water is expected to appear, whereas the original water populations are expected to decrease. The decreasing water populations are mainly detected by measurement of the cheese sample above the serum layer (Figure 4a). The newly appearing water population can be detected by adjusting the position of the sample tube in the NMR spectrometer using a 30 mm height Teflon spacer, which enables the

analysis of the cheese surrounded by the separated layer (Figure 4d).

The FID and CPMG relaxation characteristics of the mozzarella plug above the serum layer are shown in Figure 4b,c, respectively. Upon loss of serum from mozzarella, the integrated amplitude ( $A$ ) of the total FID-signal decreased, which was mainly due to a decrease of  $A$  related to liquid phase protons in the plug above the serum layer (i.e., peak at  $T_2^* > 26 \mu\text{s}$ ). Note that the  $A$  value of the relaxation component  $H_{\text{solid fat}}$  hardly changed upon heating and cooling (i.e.,  $395 \pm 0$  vs.  $408 \pm 1$  a.u.). Before and after incubation at 30°C, the CPMG experiment on fresh mozzarella yielded a third peak at  $T_2 > 60$  ms (labelled as “ $H_{\text{water in fresh mozz}}$ ”). The comparison with aged cheese (Figures 1 and 2) indicates that the latter peak with longer relaxation times must be linked with water protons that do not interact with macromolecules within the cheese matrix to the same extent yet. Additional analyses at

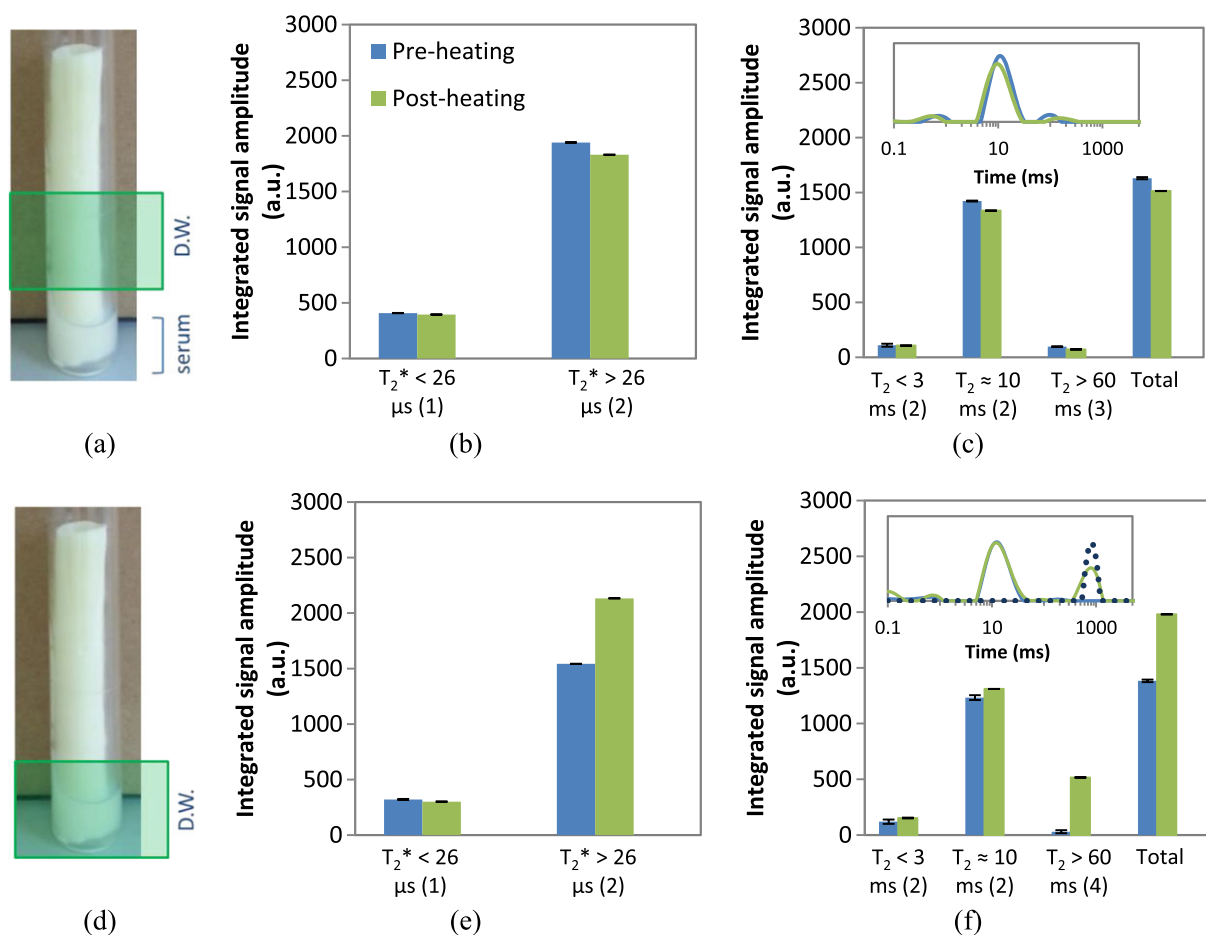


**FIGURE 4** (a,d) Detection window (D.W.; about 26 mm in height) of the Maran Ultra 23 spectrometer (Oxford Instruments, UK) without and with the use of a 30 mm height Teflon spacer, respectively. FID (b,e) and CPMG (c,f) characteristics of fresh mozzarella as measured above the serum layer at 5°C (b,c) and as surrounded by serum (e,f). The insets show the CPMG-based  $T_2$  relaxation time distribution of the mozzarella before (blue line) and after mild heating (green line). The blue dotted line refers to bulk serum. 1 =  $H_{\text{solid fat}}$ ; 2 =  $H_{\text{liquid oil + water}}$ ; 3 =  $H_{\text{water in fresh mozz}}$ ; 4 =  $H_{\text{released water}}$ .



intermediary time points showed that the fraction decreases with increasing storage time (data not shown). Figure 4c shows that the  $A$  value of the total CPMG-signal decreased after the mild heat treatment (with about 116 a.u.), which was reflected in a decrease of the signal of  $H_{\text{water in fresh mozz}}$  (with about 26 a.u.) and of the major peak at  $T_2$  of about 10 ms (with about 87 a.u.). There was no change in the signal for the relaxation component with  $T_2 < 3$  ms, which indicates that the heat-releasable serum was associated with the (two) peaks with  $T_2$  times longer than 3 ms. The  $T_2$  relaxation time of the peak at  $T_2 = 10$  ms slightly decreased from  $10.9 \pm 0.0$  to  $9.6 \pm 0.0$  ms upon mild heat treatment, which might indicate that the releasable serum originates from the second half of the major peak. In the latter case, serum release then results in a shift of the remaining major peak to shorter relaxation times. Combining the findings from the heating experiments on EFP and mozzarella, the proton pool characterized by a relaxation time that ranges between a few milliseconds and less than 60 ms can be ascribed to the liquid fraction of the fat phase, as well as to water protons ( $H_{\text{liquid oil + water}}$ ). These water protons experience more interaction with the cheese matrix as compared with the weakly interacting water population  $H_{\text{water in fresh mozz}}$ .

The possibility to detect differences between fresh and aged low-moisture mozzarella allows future studies to be conducted on production and/or storage parameters affecting the cheese-ripening process.

The FID and CPMG relaxation characteristics of the mozzarella plug surrounded by a serum layer, as well as of the bulk serum, are depicted in Figure 4e,f,

respectively. Based on the CPMG experiment, the  $T_2$  relaxation time of the bulk serum amounted to 798 ms, which is equal to the newly appeared CPMG-peak of mozzarella surrounded by serum, and hence, this relaxation component is associated with protons of the released serum ( $H_{\text{released water}}$ ). As compared with water within the mozzarella, the released serum experiences much less surface interactions, and hence, it is characterized by a longer relaxation time. The new peak resulted in an increase of the integrated amplitude of the total CPMG signal (Figure 4f). Remarkably, the  $A$  value of the major peak at  $T_2 = 10$  ms and of the minor peak at  $T_2 < 3$  ms increased (from  $1233 \pm 22$  to  $1310 \pm 1$  a.u. and from  $120 \pm 20$  to  $153 \pm 4$  a.u., respectively), which might be due to some extent of water absorption by the mozzarella matrix. In accordance with the CPMG findings, the total intensity of the FID signal increased due to an increase in intensity of the liquid signal (Figure 4e). As compared with the  $A$  value of  $H_{\text{solid fat}}$  before heating ( $321 \pm 5$  a.u.), the peak area did not increase after heating and cooling back to  $5^\circ\text{C}$  ( $301 \pm 3$  a.u.), indicating that the released serum was fat free.

### 3.7 | Addition of deuterated water to mozzarella

In a fourth approach, a  $\text{D}_2\text{O}$  phase was added to aged mozzarella cheese. At different time points (i.e., after a few minutes, 3 and 6 hr), a CPMG (Figure 5) and FID-CPMG experiment (Figure 6) was performed.

Hereby, the bulk  $\text{D}_2\text{O}$  phase is not detected by  $^1\text{H}$  NMR (base line in Figure 5a). Upon exchange between

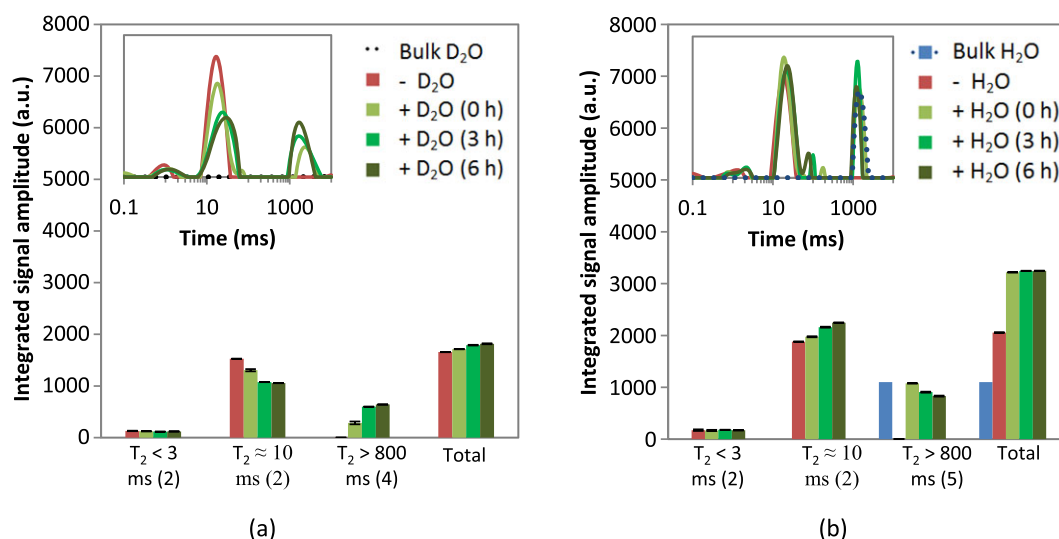


**FIGURE 5** The Carr–Purcell–Meiboom–Gill-based  $T_2$  relaxation time distribution of aged mozzarella to which a  $\text{D}_2\text{O}$  phase (a) and a  $\text{H}_2\text{O}$  phase (b) was added. The black (a) and blue (b) dotted lines refer to a bulk  $\text{D}_2\text{O}$  and bulk  $\text{H}_2\text{O}$  phase, respectively. 2 =  $H_{\text{liquid oil + water}}$ ; 4 =  $H_{\text{released water}}$ ; 5 =  $H_{\text{added water}}$

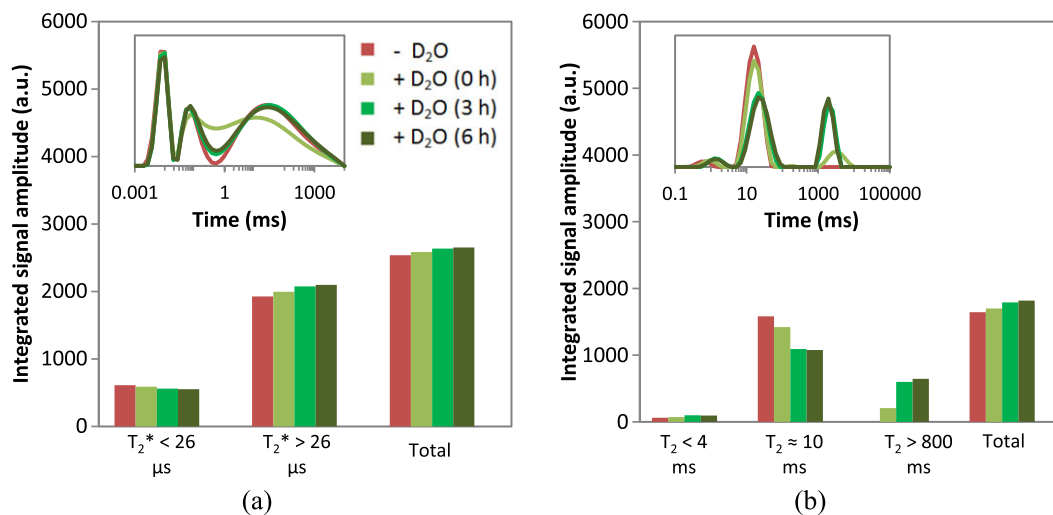


**FIGURE 6** Free-induction decay-based  $T_2^*$  (a) and Carr–Purcell–Meiboom–Gill-based  $T_2$  (b) relaxation time distribution characteristics of aged mozzarella with (0, 3 and 6 hours) and without addition of a  $D_2O$  phase

expressible mozzarella water (i.e., water that is not entrapped in fully confined compartments) and (bulk)  $D_2O$  phase, part of the expressible mozzarella water is released by which two phenomena are expected. First, the peak area of the relaxation component related to expressible mozzarella water is expected to decrease (part of the water is replaced by  $D_2O$ ). Second, an additional relaxation component is expected to appear, as the relaxation time of the released water is expected to be longer than for internal water.

Figure 5a shows that the  $A$  value of the major relaxation peak (with  $T_2$  of about 10 ms) significantly decreased directly upon addition of  $D_2O$  ( $p < 0.02$ ). As was the case for the heat-expressible water protons, also the  $D_2O$ -expressible water protons originated from the dominant CPMG-peak. The largest decrease seemed to occur in less than 3 hr after  $D_2O$  addition. On the other hand, a new relaxation component with  $T_2 = 1.3$  s ( $H_{\text{released water}}$ ) appeared upon addition of the  $D_2O$  phase. Hereby, the long relaxation time indicates that the released water from mozzarella behaves like bulk water. Recall that the heat-induced released serum was characterized by a  $T_2$  time of about 0.8 s; the longer  $T_2$  relaxation time for  $D_2O$ -expressible water follows from the effect of dilution. The significant increase in the total signal amplitude (by about 6%) for mozzarella in contact with  $D_2O$  as a function of storage time (from 0 up to 6 hr, with  $p < 0.02$ ) might indicate the release of very fast relaxing water from mozzarella (i.e., too fast to be detected by the CPMG experiment).

The control treatment consisted of the addition of a water phase to a mozzarella plug. The expressible mozzarella water is exchanged with the added  $H_2O$  phase, whereby the redistribution of  $H_2O$  is only expected to

result in the appearance of a new relaxation peak related to bulk water (in fact, a mixture of mozzarella water and added  $H_2O$  phase), which is located at  $T_2 = 1.4$  s (“ $H_{\text{added water}}$ ”) in Figure 5b. However, Figure 5b shows that there was an increase of the signal amplitude of the major relaxation component at a  $T_2$  of about 10 ms (and a decrease in signal at  $T_2 > 800$  ms). This indicates some extent of water absorption of the mozzarella, which corresponds to the findings from the experiment on mozzarella surrounded by heat-induced released serum. The broadening of the major relaxation peak upon addition of the  $H_2O$  phase illustrates that the interaction of the absorbed water with macromolecules is less strong.

The total integrated amplitude of the CPMG-signal of mozzarella mixed with the  $H_2O$  phase ( $3,217 \pm 3$  a.u. at 0 hr contact time) was in agreement with the sum of the signals coming from the bulk  $H_2O$  phase (about 1,100 a.u.) and from mozzarella ( $2,055 \pm 9$  a.u. without  $H_2O$  phase).

The hypothesis that there exists a fraction of very fast relaxing water in mozzarella (i.e., too fast to be detected by the CPMG experiment) was examined by running the FID-CPMG sequence. Figure 6a,b shows the change in the  $T_2^*$  relaxation time distribution for mozzarella mixed with  $D_2O$  phase as obtained from the FID-part and CPMG-part of the FID-CPMG experiment, respectively.

The total signal intensity of the CPMG-part of the FID-CPMG experiment increased (by about 7%, Figure 6 b) from 0 to 6 hr after  $D_2O$  addition, which was consistent with the increase in area of the FID-peak at  $T_2^* > 26 \mu\text{s}$  in Figure 6a, as well as with the increase in total CPMG-signal in Figure 5a. At the same time, the peak area at  $T_2^* < 26 \mu\text{s}$  decreased (by about 6%) as a function of

D<sub>2</sub>O contact time. Hence, these observations sustain the hypothesis that the relaxation component at  $T_2^* < 26 \mu\text{s}$  is not only associated with the solid fraction of the fat phase but also with some very strongly interacting water. This implies that the difference in SFC between bulk EFP and mozzarella will even be larger.

## 4 | CONCLUSIONS

Fresh and aged low-moisture mozzarella were analyzed using time-domain NMR  $T_2$  relaxometry. The objective was to improve the interpretation of the experimentally determined  $T_2$  relaxation time distribution.

The FID-CPMG and CPMG sequence were applied, and the generated data were fitted using CONTIN analysis. The CPMG sequence provided details about the relaxation behavior of protons from the liquid phase, whereas the FID-CPMG sequence offered additional details related to protons from the solid fat phase.

The shortest relaxation times were found to be linked to solid fat protons, as well as to very strongly interacting water protons. The CPMG-experiment on aged mozzarella revealed different relaxation peaks, all of which were assigned to both liquid oil protons and water protons that interact with the protein matrix. Fresh mozzarella yielded an extra relaxation peak (with longer relaxation times) that was ascribed to weakly interacting water protons.

Application of a mild heat treatment or the addition of deuterated water generated a rearrangement of the proton pools. Both stimuli promoted the release of water from either fresh or aged mozzarella, resulting in the appearance of a new relaxation peak (with even longer relaxation times). Furthermore, there were indications that some extent of water absorption occurred when mozzarella was in contact with water.

In future research, the proposed NMR sequences may be applied for evaluation of the effect of process and formulation aspects on the behavior of the water fractions in low-moisture mozzarella.

## ACKNOWLEDGEMENTS

We would like to express our gratitude to Dirk Van Gaver (Milcobel cvba) and Timothy P. Guinee (Teagasc Food Research Centre, Cork, Ireland) for the fruitful scientific discussions. The research was funded by Flanders Innovation & Entrepreneurship (Grant HBC.2017.0297, VLAIO, Belgium). L. V., A. D., and P. V. d.M. thank the Fund for Scientific Research—Flanders (FWO-Vlaanderen) for their financial support for obtaining the time-domain NMR equipment.

## CONFLICT OF INTEREST

There are no conflicts of interest.

## ORCID

Lien Vermeir  <https://orcid.org/0000-0002-9768-8010>

## REFERENCES

- [1] G. Gernigon, P. Schuck, R. Jeantet, *Dairy Sci. Technol.* **2010**, *90*, 27.
- [2] M. A. E. Auty, M. Twomey, T. P. Guinee, D. M. Mulvihill, *J. Dairy Res.* **2001**, *68*, 417.
- [3] H. M. Lilbæk, M. L. Broe, E. Høier, T. M. Fatum, R. Ipsen, N. K. Sørensen, *J. Dairy Sci.* **2006**, *89*, 4114.
- [4] J. R. Smith, J. P. Hindmarsh, A. J. Carr, M. D. Golding, D. Reid, *J. Food Eng.* **2013**, *214*, 257.
- [5] V. Banville, D. Chabot, N. Power, Y. Pouliot, M. Britten, *Int. Dairy J.* **2016**, *61*, 155.
- [6] X. Ma, B. James, L. Zhang, E. A. C. Emanuelsson-Patterson, *J. Food Eng.* **2013**, *115*, 154.
- [7] P. Sharma, P. A. Munro, G. Gillies, P. G. Wiles, *LWT—Food Sci. Technol.* **2017**, *83*, 184.
- [8] I. Hussain, A. S. Grandison, A. E. Bell, *Food Chem.* **2012**, *134*, 1500.
- [9] M. El-Bakry, J. Sheehan, *J. Food Eng.* **2014**, *125*, 84.
- [10] D. J. McMahon, R. L. Fife, C. J. Oberg, *J. Dairy Sci.* **1999**, *82*, 1361.
- [11] M.-I. Kuo, S. Gunasekaran, M. Johnson, C. Chen, *J. Dairy Sci.* **2001**, *84*, 1950.
- [12] M. R. Guo, P. S. Kindstedt, *J. Dairy Sci.* **1995**, *78*, 2099.
- [13] M.-I. Kuo, M. E. Anderson, S. Gunasekaran, *J. Dairy Sci.* **2003**, *86*, 2525.
- [14] R. Gianferri, M. Maioli, M. Delfini, E. Brosio, *Int. Dairy J.* **2007**, *17*, 167.
- [15] R. Anedda, Magnetic resonance analysis of dairy processing: suitable tools for the dairy industry, in *Magnetic Resonance in Food Science*, (Eds: F. Capozzi, L. Laghi, P. S. Belton), The Royal Society of Chemistry, Cambridge **2015**.
- [16] B. P. Hills, S. F. Takacs, P. S. Belton, *Food Chem.* **1990**, *37*, 95.
- [17] A. Altan, M. H. Oztop, K. L. McCarthy, M. J. McCarthy, *J. Food Eng.* **2011**, *107*, 200.
- [18] S. M. Møller, T. B. Hansen, U. Andersen, S. K. Lillevang, A. Rasmussen, H. C. Bertram, *J. Agric. Food Chem.* **2012**, *60*, 1635.
- [19] D. Cais-Sokolińska, P. Bierzuńska, Ł. K. Kaczyński, H. M. Baranowska, J. Tomaszewska-Gras, *J. Food Eng.* **2018**, *222*, 226.
- [20] C. M. Andersen, M. B. Frøst, N. Viereck, *Int. Dairy J.* **2010**, *20*, 32.
- [21] B. Chaland, F. Mariette, P. Marchal, J. De Certaines, *J. Dairy Res.* **2000**, *67*, 609.
- [22] S. Meiboom, D. Gill, *Rev. Sci. Instrum.* **1958**, *29*, 688.
- [23] A. Declerck, V. Nelis, T. Rimaux, K. Dewettinck, P. Van der Meer, *Eur. J. Lipid Sci. Technol.* **2017**, *120*, 1700339.
- [24] D. Le Botlan, I. Helie-Fourel, *Anal. Chim. Acta* **1995**, *311*, 217.

- [25] R. R. Ruan, P. L. Chen, *Water in Foods and Biological Materials: A Nuclear Magnetic Resonance Approach*, CRC Press, Boca Raton **1998**.
- [26] S. W. Provencher, *Comput. Phys. Commun.* **1982**, *27*, 213.
- [27] S. W. Provencher, *Comput. Phys. Commun.* **1982**, *27*, 229.
- [28] N. Noronha, E. Duggan, G. R. Ziegler, E. D. O'Riordan, M. O'Sullivan, *Food Hydrocoll.* **2008**, *22*, 1612.
- [29] M. El-Bakry, E. Duggan, E. D. O'Riordan, M. O'Sullivan, *LWT—Food Sci. Technol.* **2010**, *43*, 1079.
- [30] S. M. Møller, H. C. Bertram, U. Andersen, S. K. Lillevang, A. Rasmussen, T. B. Hansen, *Food Microbiol.* **2013**, *36*, 90.
- [31] P. C. Belsito, M. V. S. Ferreira, L. P. Cappato, R. N. Cavalcanti, V. A. S. Vidal, T. C. Pimentel, E. A. Esmerino, C. F. Balthazar, R. P. C. Neto, M. I. B. Tavares, P. B. Zacarchenco, M. Q. Freitas, M. C. Silva, R. S. L. Raices, G. M. Pastore, M. A. R. Polonio, A. G. Cruz, *Carbohydr. Polym.* **2017**, *174*, 869.
- [32] D. F. da Silva, F. H. Larsen, A. B. Hougaard, R. Ipsen, *Int. Dairy J.* **2017**, *74*, 27.
- [33] M. F. Sperry, H. L. A. Silva, C. F. Balthazar, E. A. Esmerino, S. Verruck, E. S. Prudencio, R. P. C. Neto, M. I. B. Tavares, J. C. Peixoto, F. Nazarro, R. S. Rocha, J. Moraes, A. S. G. Gomes, R. S. L. Raices, M. C. Silva, D. Granato, T. C. Pimentel, M. Q. Freitas, A. G. Cruz, *J. Funct. Foods* **2018**, *45*, 435.
- [34] B. K. S. Khanal, B. Bhandari, S. Prakash, D. Liu, P. Zhou, N. Bansal, *Food Hydrocoll.* **2018**, *83*, 97.
- [35] S. J. Vogt, J. R. Smith, J. D. Seymour, A. J. Carr, M. D. Golding, S. L. Codd, *J. Food Eng.* **2015**, *150*, 35.
- [36] H. M. Baranowska, J. Tomaszewska-Gras, D. Cais-Sokolińska, P. Bierzuńska, L. L. Kaczyński, *Mljekarstvo* **2017**, *67*, 188.
- [37] J. R. Smith, S. J. Vogt, J. D. Seymour, A. J. Carr, S. L. Codd, *J. Food Eng.* **2017**, *198*, 1.
- [38] K. Smet, J. De Block, P. Van der Meeren, K. Raes, K. Dewettinck, K. Coudijzer, *Dairy Sci. Technol.* **2010**, *90*, 431.
- [39] J. M. deMan, *Food Microstructure* **1982**, *1*, 209.
- [40] T. R. Nelson, S. M. Tung, *Magn. Reson. Imaging* **1987**, *5*, 189.
- [41] D. H. Gultekin, J. C. Gore, *J. Magn. Reson.* **2005**, *172*, 133.

**How to cite this article:** Vermeir L, Declerck A, To CM, Kerkaert B, Van der Meeren P. Water and oil signal assignment in low-moisture mozzarella as determined by time-domain NMR  $T_2$  relaxometry. *Magn Reson Chem.* 2019;57:674–685. <https://doi.org/10.1002/mrc.4842>